Energy Proceedings
Vol 41, 2024
ISSN 2004-2965

Direct quantification of anthropogenic CO_2 emissions: Insights from Satellite Observations

Bo Huang[1*], Jia He [1]

1 Department of Geography, The University of Hong Kong

(*Corresponding Author: bohuang@hku.hk)

ABSTRACT

Carbon dioxide (CO_2) contributes to over 50% of the enhanced radiative forcing, which in turn leads to climate change. Regular monitoring of CO_2 emissions is commonly required by various governments for strategic management purposes. However, the conventional self-reporting mechanism heavily relies on reporting parties, making it less efficient and subjective. This study proposes a direct method to estimate the CO_2 emissions using satellite-based column-averaged mole fractions of CO_2 (XCO_2) retrievals. To account for spatial and temporal variability, the study adopts the geographically and temporally weighted regression (GTWR) model. The results show high consistency, indicating the potential of using satellite-based data to track anthropogenic emissions with more frequent and extensive coverage.

Keywords: CO_2 emissions, XCO_2, OCO-2, GTWR

NONMENCLATURE

Abbreviations	
AT	Air Temperature
CO_2	Carbon dioxide
GHG	Greenhouse Gas
GTWR	Geographically and Temporally Weighted Regression
MB	Mean Bias
OCO-2	Orbiting Carbon Observatory-2
TCWV	Total Column Water Vapor
UNFCCC	UN Framework Convention on Climate Change
WS	Wind Speed
XCO_2	column averaged CO_2 dry air mole fraction of CO_2

1. INTRODUCTION

The concentration of CO_2 has steadily risen in the past few decades as a result of human activities, especially from fossil fuel combustions [1]–[3]. To foster a sustainable low-carbon economy, the Paris Agreement of UN Framework Convention on Climate Change (UNFCCC) mandates the monitoring of anthropogenic greenhouse gas (GHG) emissions and the implementation of mitigation commitments to reduce carbon emissions. It is crucial for governments to have reliable statistics on CO_2 emissions to assess progress in mitigation efforts [4].

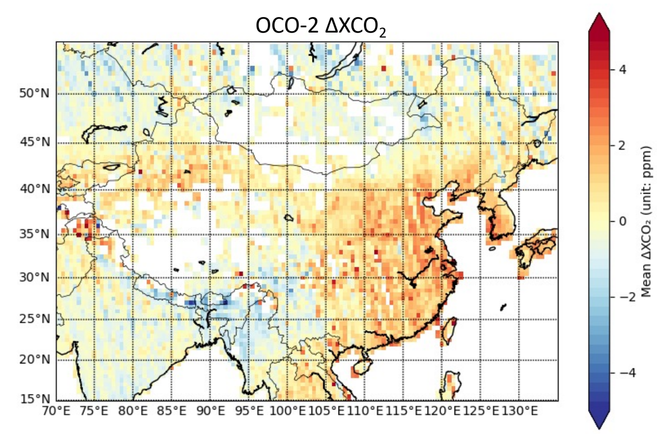

Fig. 1. Mean of ΔXCO_2 data obtained from OCO-2 during 201409 – 201912.

Ground-based observations offer a comprehensive understanding of the growth rate and variation trends of atmospheric CO_2 [5], [6]. However, sparse nature of the observation network limits the accurate inference of global-scale carbon emissions. “Bottom-up” inventories are fundamental for managing CO_2 emissions at various levels, but their quality varies among and within reporting parties [7], [8]. The conventional “top-down” approach often relies on satellite measurements as proxies to disaggregate consumption statistics, which

This is a paper for 15th International Conference on Applied Energy (ICAE2023), Dec. 3-7, 2023, Doha, Qatar.

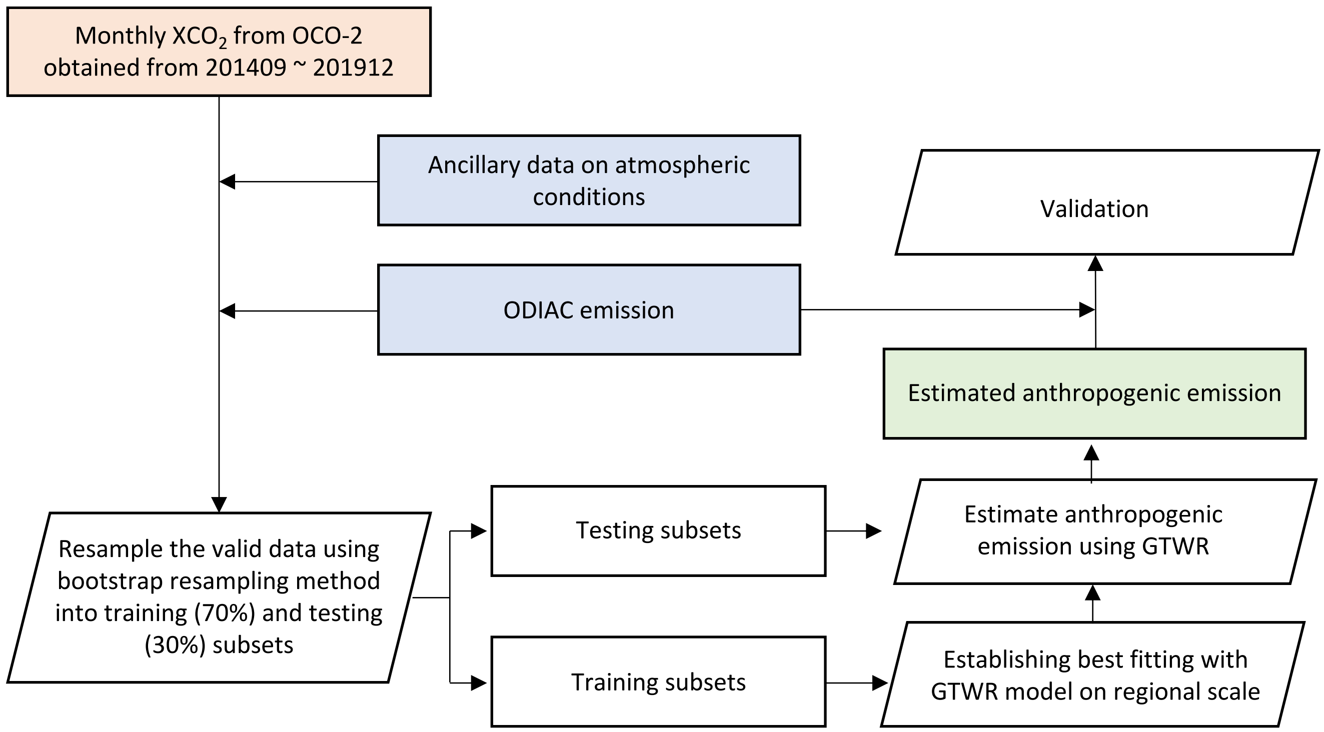

Fig. 2. Flowchart of anthropogenic emissions estimation using ΔXCO_2 data obtained from OCO-2

poses challenges in ensuring the accuracy and consistency of estimation results [9].

Satellite-based remote sensing observations offer additional measurements to the existing surface-based greenhouse gas monitoring network, enabling the estimation of surface fluxes of CO_2 and other greenhouse gases on regional scales worldwide [10], [11]. The column averaged CO_2 dry air mole fraction of CO_2 (XCO_2) was calculated using data from various satellite missions to estimate anthropogenic emissions [12], [13]. For example, cluster analysis was performed on the enhanced XCO_2 (ΔXCO_2) extracted from the Orbiting Carbon Observatory-2 (OCO-2), revealing a positive correlation between CO_2 and emission inventories [14]. Multiple linear regression model [15] and general regression neural network model were proposed to estimate anthropogenic CO_2 emissions from satellite-based observations.

Despite decades of research on carbon monitoring, significant uncertainties persist in measuring global carbon emissions. Here a reliable estimation on atmospheric CO_2 emission was proposed to estimate global anthropogenic emissions with multi-year XCO_2 data extracted from OCO-2. Moreover, the geographically and temporally weighted regression model is utilized to simulate the relationship between ΔXCO_2 and anthropogenic emissions with localized correction [16]. The main goal of this study is to develop an objective approach to directly estimate CO_2 emissions from satellite-based measurement on CO_2 amount.

2. MATERIALS

2.1 XCO_2

NASA's OCO-2 is one of the most popular satellites designed to monitor CO_2 variations from space [17], [18]. It was launched into a sun-synchronous orbit in 2014, aiming to reduce uncertainties in the spatial-temporal distribution of biospheric carbon fluxes on regional scales. It measures the solar backscattered radiance in the near infrared (NIR) and shortwave infrared (SWIR), including the O_2-A band at 760 nm, the weak CO_2 band at around 1610 nm, and the strong CO2 band at around 2060 nm. The OCO-2 is operated in a near-push-broom style with a spatial resolution at around 1.29 km x 2.25 km [18]. The validation on OCO-2 XCO_2product against ground-based Total Carbon Column Observing Network (TCCON) indicate an uncertainty of 1.3 ppm [19]. Here we adopted the OCO-2 L2 bias-corrected XCO_2 product (OCO2_L2_Lite_FB_10r) and re-grided to a spatial resolution of 0.02 x 0.02 degrees future analysis.

2.2 Ancillary data

The atmospheric conditions, such as total column water vapor (TCWV), air temperature (AT), local wind speed (WS), and vertical velocity from ERA5 were obtained as ancillary data in the estimation process.

ERA5 is the global climate and weather reanalysis developed by the European Centre for Medium-Range Weather Forecasts (ECMWF), and it integrates model simulations with observational data [20]. The local wind field was employed to account for the atmospheric movement in the horizontal direction. More specifically, the average wind speeds (WS) at 1000, 975, and 950 hPa were calculated to approximate the wind below 500 m [21].

Large-scale atmospheric circulation is another driving force for regional changes of atmospheric concentration. The vertical velocity at 500 hPa (ω500) was utilized as the proxy of large-scale circulation [22].

The bottom-up inventory of CO_2 emissions of ODIAC is a global high-resolution emissions data product for fossil fuel carbon dioxide emissions commonly adopted as reference data on CO_2 emissions [23]. This dataset utilizes datasets from multiple resources, including energy statistics, emissions inventories, and satellite observations, to provide detailed picture of CO_2 emissions. The ODIAC were employed as a reference for CO_2 emissions for model development and validation analysis.

Notably, all datasets were re-grided into 0.02 x 0.02 degrees to align with the data obtained from remote sensing satellite.

3. METHODOLOGY

This study proposed a direct estimation approach to anthropogenic CO_2 emissions with XCO_2 data obtained from OCO-2.

While the anthropogenic emissions only account for a small percentage of carbon fluxes, identifying the CO_2 fluxes arising from natural sources and anthropogenic emissions is critical. To enhance the observation signals and isolate the anthropogenic emissions from CO_2 columns, the monthly median from the study area was subtracted as the background CO_2 fluxes [14]. The XCO_2 anomaly (ΔXCO_2) was derived as follows:

$$\Delta XCO_2 = XCO_2(individual) - XCO_2(monthly\ median) \quad (1)$$

This step detrends the XCO_2 data while reducing the impact of potential regional-scale biases in the OCO-2 product.

Atmospheric transport is one of the most critical elements in estimating CO_2 emissions. In this study, the wind speed is utilized to indicate the atmospheric movement in the horizontal directions, and the vertical velocity is used to identify the atmospheric movement in the vertical directions. In addition, the near-surface air temperature and humidity are also included in the model development.

To capture the spatiotemporal heterogeneity between ΔXCO_2 and CO_2 emissions, the geographically and temporally weighted regression (GTWR) model is adopted in this research [16]. The model estimates local regression coefficients for each observation by considering the neighboring observations within a specified bandwidth. This allows for the modeling of spatially varying relationships between the variables. The estimation model could be expressed as:

$$\begin{aligned} AE_i = \beta_0(\mu_i, \nu_i, t_i) &+ \beta_1(\mu_i, \nu_i, t_i) \times \Delta XCO_{2i} \\ &+ \beta_2(\mu_i, \nu_i, t_i) \times \omega 500_i \\ &+ \beta_3(\mu_i, \nu_i, t_i) \times WS_i \\ &+ \beta_4(\mu_i, \nu_i, t_i) \times AT_i \\ &+ \beta_5(\mu_i, \nu_i, t_i) \times TCWV_i + \varepsilon_i \end{aligned} \quad (2)$$

where AE_i are the monthly anthropogenic emissions of sample i at location (μ_i, ν_i) at time t_i. β_0 is the intercept at location (μ_i, ν_i) at time t_i. β_1–β_5 denote the location-and-time-specific slopes for ΔXCO_2 observed from OCO-2, ω500, WS, AT, and TCWV, respectively. ε_i represents the offset.

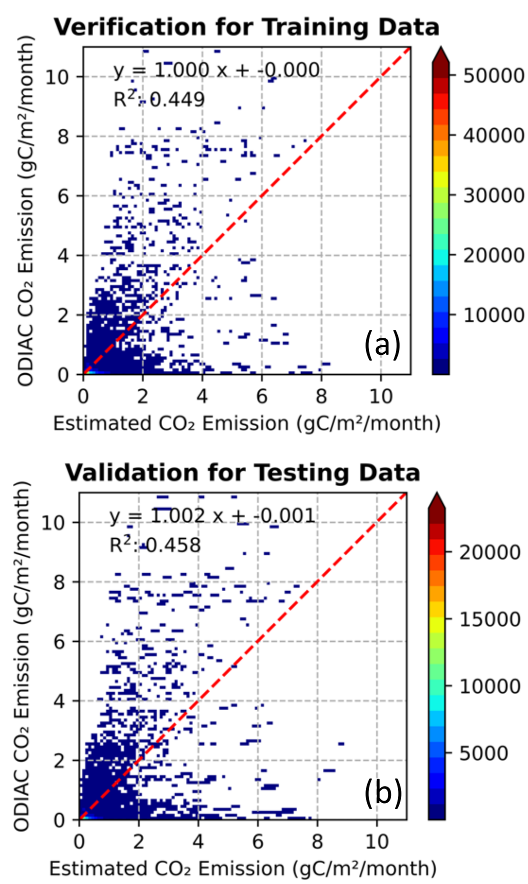

Fig. 3. Scatter plot of anthropogenic emissions estimated from OCO-2 and the collocated ODIAC product from 201409 to 201912 for (a) the training dataset and (b) the testing dataset.

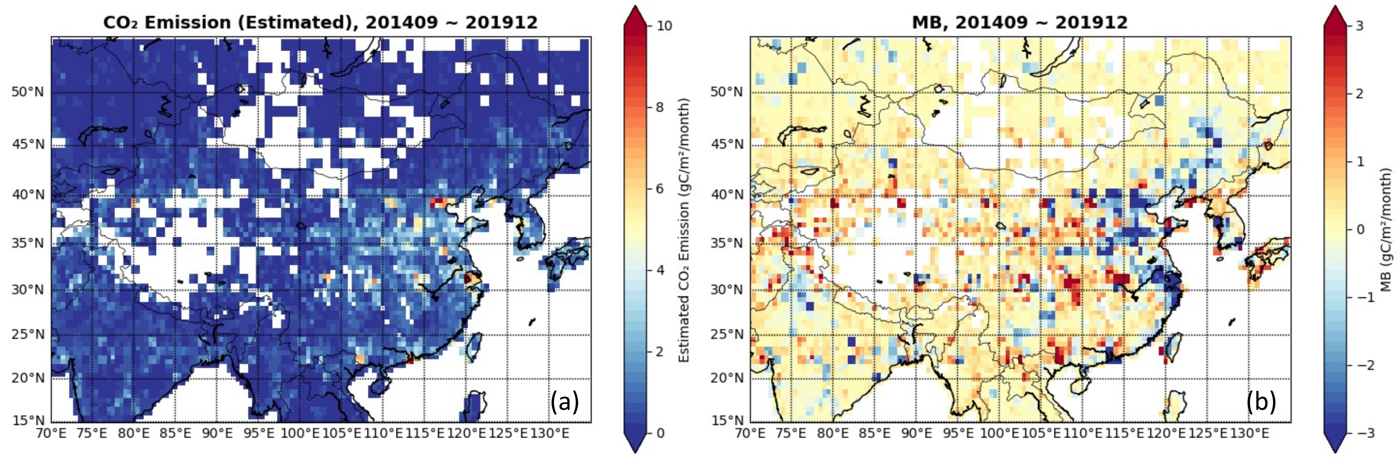

Fig. 4. *Distribution map of the (a) estimated CO_2 emission* obtained from OCO-2 during 201409 – 201912, (b) mean bias between satellite-based estimation and ODIAC data.

A total of 2,894,275 groups of valid collocated samples are obtained during the observation period at the research area (latitude: 15 °N ~ 55 °N，longitude: 70 °E ~ 135 °E). The bootstrap resampling method is used to separate the dataset into subsets for model training (~70%, 315,000 samples) and testing (~30%, 135,954 samples). The purpose of this resampling step was to align datasets into separate training and testing subsets, ensuring independence, and minimizing the influence of the diverse spatial distribution of data points and potential biases in satellite observations.

4. RESULTS AND DISCUSSIONS

The monthly anthropogenic emissions are estimated using the GTWR model with the ΔXCO_2 extracted from OCO-2 XCO_2 product. To reduce the computational time and computer memory, the analysis was conducted with spatial resolution of 0.5 degree.

The cross validation is conducted for the newly estimated dataset. The scatter plots of CO_2 emissions from satellite-based estimation and the collocated ODIAC product from 201409 to 201912 are presented in Figure 3. The R^2 for the training and testing subsets are 0.449 and 0.458, respectively.

The characteristics of CO_2 emission are investigated using the estimated data. The mean bias (MB) between the satellite-based estimation and the ODIAC inventory are calculated:

$$MB = \frac{1}{n}\sum_{i=1}^{n}(AE_{estimated} - AE_{ODIAC}) \quad (3)$$

where n denotes the number of sample size, the $AE_{estimated}$ is the estimation results, and the AE_{ODIAC} is the data obtained from ODIAC inventory.

As the distribution map of satellite-based estimation shown in Figure 4 (a), emission hotspots are observed in areas such as the Beijing-Tianjin-Hebei province cluster and Yangtze River Delta area. The MB shown in Figure 4 (b) indicate overestimation in central China and underestimation in eastern China.

To summarize, this study successfully demonstrated a practical technique for direct estimating CO_2 emissions using satellite-based observations of column amount CO_2. The validation results indicate that the proposed estimation approach is reliable, both in terms of spatial and temporal aspects. These findings are significant for the utilization of CO_2 satellite data in independently monitoring CO_2 emissions at different levels.

ACKNOWLEDGEMENT

This work was supported by the National Key Research and Development Program of China (2022YFB3903700 and 2019YFC1510400), the Research Grants Council of Hong Kong (AoE/E-603/18), and the National Natural Science Foundation of China (No. 42271439). The XCO_2 data were obtained from OCO-2 project (https://disc.gsfc.nasa.gov/datasets?keywords=oco3). The ancillary data on atmospheric conditions were obtained from the European Centre for Medium-Range Weather Forecasts (ECMWF) ERA5 reanalysis products (https://cds.climate.copernicus.eu). The ODIAC CO2 emissions (https://db.cger.nies.go.jp/dataset/ODIAC/DL_odiac2020b.html) provided by the Center for Global Environmental Research (CGER) at NIES.

DECLARATION OF INTEREST STATEMENT

The authors declare that they have no known competing financial interests or personal relationships that could have appeared to influence the work reported in this paper. All authors read and approved the final manuscript.

REFERENCE

[1] P. Friedlingstein *et al.*, “Global Carbon Budget 2021,” *Earth Syst. Sci. Data Discuss.*, pp. 1–191, Nov. 2021, doi: 10.5194/essd-2021-386.

[2] P. Friedlingstein *et al.*, “Global Carbon Budget 2019,” *Earth Syst. Sci. Data*, vol. 11, no. 4, pp. 1783–1838, Dec. 2019, doi: 10.5194/essd-11-1783-2019.

[3] O. Schneising, M. Buchwitz, M. Reuter, J. Heymann, H. Bovensmann, and J. P. Burrows, “Long-term analysis of carbon dioxide and methane column-averaged mole fractions retrieved from SCIAMACHY,” *Atmospheric Chem. Phys.*, vol. 11, no. 6, pp. 2863–2880, Mar. 2011, doi: 10.5194/acp-11-2863-2011.

[4] Y. Xu, *Environmental Policy and Air Pollution in China: Governance and Strategy (Edition 1)*. Routledge, 2020. doi: 10.4324/9780429452154.

[5] S. Solomon, G.-K. Plattner, R. Knutti, and P. Friedlingstein, “Irreversible climate change due to carbon dioxide emissions,” *Proc. Natl. Acad. Sci.*, vol. 106, no. 6, pp. 1704–1709, Feb. 2009, doi: 10.1073/pnas.0812721106.

[6] B. C. O’Neill *et al.*, “Demographic change and carbon dioxide emissions,” *The Lancet*, vol. 380, no. 9837, pp. 157–164, Jul. 2012, doi: 10.1016/S0140-6736(12)60958-1.

[7] C. Le Quéré *et al.*, “Temporary reduction in daily global CO2 emissions during the COVID-19 forced confinement,” *Nat. Clim. Change*, vol. 10, no. 7, Art. no. 7, Jul. 2020, doi: 10.1038/s41558-020-0797-x.

[8] Z. Liu *et al.*, “Near-real-time monitoring of global CO2 emissions reveals the effects of the COVID-19 pandemic,” *Nat. Commun.*, vol. 11, no. 1, Art. no. 1, Oct. 2020, doi: 10.1038/s41467-020-18922-7.

[9] T. Oda *et al.*, “Errors and uncertainties in a gridded carbon dioxide emissions inventory,” *Mitig. Adapt. Strateg. Glob. Change*, vol. 24, no. 6, pp. 1007–1050, Aug. 2019, doi: 10.1007/s11027-019-09877-2.

[10] S. Crowell *et al.*, “The 2015–2016 carbon cycle as seen from OCO-2 and the global in situ network,” *Atmospheric Chem. Phys.*, vol. 19, no. 15, pp. 9797–9831, Aug. 2019, doi: 10.5194/acp-19-9797-2019.

[11] A. J. Cogan *et al.*, “Atmospheric carbon dioxide retrieved from the Greenhouse gases Observing SATellite (GOSAT): Comparison with ground-based TCCON observations and GEOS-Chem model calculations,” *J. Geophys. Res. Atmospheres*, vol. 117, no. D21, 2012, doi: 10.1029/2012JD018087.

[12] S. Yang, L. Lei, Z. Zeng, Z. He, and H. Zhong, “An Assessment of Anthropogenic CO2 Emissions by Satellite-Based Observations in China,” *Sensors*, vol. 19, no. 5, p. 1118, Mar. 2019, doi: 10.3390/s19051118.

[13] M. Reuter *et al.*, “Decreasing emissions of NOx relative to CO2 in East Asia inferred from satellite observations,” *Nat. Geosci.*, vol. 7, no. 11, Art. no. 11, Nov. 2014, doi: 10.1038/ngeo2257.

[14] J. Hakkarainen, I. Ialongo, and J. Tamminen, “Direct space-based observations of anthropogenic CO2 emission areas from OCO-2,” *Geophys. Res. Lett.*, vol. 43, no. 21, p. 11,400-11,406, 2016, doi: 10.1002/2016GL070885.

[15] G. Pan, Y. Xu, and B. Huang, “Evaluating national and subnational CO2 mitigation goals in China’s thirteenth five-year plan from satellite observations,” *Environ. Int.*, vol. 156, p. 106771, Nov. 2021, doi: 10.1016/j.envint.2021.106771.

[16] B. Huang, B. Wu, and M. Barry, “Geographically and temporally weighted regression for modeling spatio-temporal variation in house prices,” *Int. J. Geogr. Inf. Sci.*, vol. 24, no. 3, pp. 383–401, Mar. 2010, doi: 10.1080/13658810802672469.

[17] D. Crisp *et al.*, “The Orbiting Carbon Observatory (OCO) mission,” *Adv. Space Res.*, vol. 34, no. 4, pp. 700–709, Jan. 2004, doi: 10.1016/j.asr.2003.08.062.

[18] D. Crisp *et al.*, “The on-orbit performance of the Orbiting Carbon Observatory-2 (OCO-2) instrument and its radiometrically calibrated products,” *Atmospheric Meas. Tech.*, vol. 10, no. 1, pp. 59–81, Jan. 2017, doi: 10.5194/amt-10-59-2017.

[19] M. Reuter, M. Buchwitz, O. Schneising, S. Noël, H. Bovensmann, and J. P. Burrows, “A Fast Atmospheric Trace Gas Retrieval for Hyperspectral Instruments Approximating Multiple Scattering—Part 2: Application to XCO2 Retrievals from OCO-2,” *Remote Sens.*, vol. 9, no. 11, Art. no. 11, Nov. 2017, doi: 10.3390/rs9111102.

[20] H. Hersbach *et al.*, “The ERA5 global reanalysis,” *Q. J. R. Meteorol. Soc.*, vol. 146, no. 730, pp. 1999–2049, 2020, doi: 10.1002/qj.3803.

[21] B. Zheng *et al.*, “Observing carbon dioxide emissions over China’s cities and industrial areas with the Orbiting Carbon Observatory-2,” *Atmospheric Chem. Phys.*, vol. 20, no. 14, pp. 8501–8510, Jul. 2020, doi: 10.5194/acp-20-8501-2020.

[22] J. Ma *et al.*, “Responses of the Tropical Atmospheric Circulation to Climate Change and Connection to the Hydrological Cycle,” *Annu. Rev. Earth Planet. Sci.*, vol. 46, no. 1, pp. 549–580, 2018, doi: 10.1146/annurev-earth-082517-010102.

[23] T. Oda, S. Maksyutov, and R. J. Andres, “The Open-source Data Inventory for Anthropogenic CO_2, version 2016 (ODIAC2016): a global monthly fossil fuel CO_2 gridded emissions data product for tracer transport simulations and surface flux inversions,” *Earth Syst. Sci. Data*, vol. 10, no. 1, pp. 87–107, Jan. 2018, doi: 10.5194/essd-10-87-2018.